Kinetic Energy Decay Rates of Supersonic and Super-Alfvénic Turbulence in Star-Forming Clouds

Mordecai-Mark Mac Low*, Ralf S. Klessen*, Andreas Burkert*
Max-Planck-Institut für Astronomie, Königstuhl 17, D-69117 Heidelberg, Germany

Michael D. Smith†
Astronomisches Institut der Universität Würzburg, Am Hubland, D-97074 Würzburg, Germany
(Submitted to *Phys. Rev. Letters* 28 November 1997, accepted 28 January 1998)

Abstract

We compute 3D models of supersonic, sub-Alfvénic, and super-Alfvénic decaying turbulence, with an isothermal equation of state appropriate for star-forming interstellar clouds of molecular gas. We find that in 3D the kinetic energy decays as $t^{-\eta}$, with $0.85 < \eta < 1.2$. In 1D magnetized turbulence actually decays faster than unmagnetized turbulence. We compared different algorithms, and performed resolution studies reaching 256^3 zones or 70^3 particles. External driving must produce the observed long lifetimes and supersonic motions in molecular clouds, as undriven turbulence decays too fast.

98.38.Am, 47.27.-i, 47.40.Ki, 95.30.Lz

Typeset using REVTEX

Star-forming clouds of interstellar gas emit strongly in molecular emission lines; temperatures derived from these lines show that the linewidths greatly exceed the thermal sound speed c_s in these clouds. With densities of order $n \sim 10^3 - 10^5$ protons per cm^3, the gas in these clouds can be described by an isothermal equation of state due to the efficient radiative cooling allowed by the many low-lying molecular transitions [1]. Cloud lifetimes are of order 3×10^7 yr [2], while free-fall gravitational collapse times are only $t_\mathrm{ff} = (1.4 \times 10^6 \text{ yr})(n/10^3 \text{ cm}^{-3})^{-1/2}$. In the absence of non-thermal support, these clouds should collapse and form stars in a small fraction of their observed lifetime. Supersonic hydrodynamical (HD) turbulence is suggested as a support mechanism by the observed broad lines, but was dismissed because it would decay in times of order t_ff. A popular alternative has been sub- or trans-Alfvénic magnetohydrodynamical (MHD) turbulence, which was thought to decay an order of magnitude more slowly [3]. However, analytic estimates and computational models suggest that *incompressible* MHD turbulence decays [4–7] as $t^{-\eta}$, with a decay rate $2/3 < \eta < 1.0$, while incompressible HD turbulence has been experimentally measured [8,9] to decay with $1.2 < \eta < 2$. The difference in decay rates between incompressible HD and MHD turbulence is clearly not as large as had been suggested for compressible astrophysical turbulence. In this paper we use high-resolution, three-dimensional (3D) simulations to compute the decay rates of compressible, homogeneous, isothermal, decaying turbulence with supersonic, sub-Alfénic, and super-Alfvénic root-mean-square (rms) initial velocities v_rms, and show that the decay rates in these physical regimes, $0.85 < \eta < 1.2$, strongly resemble the incompressible results.

a. Previous Work The decay of the kinetic energy E_K of incompressible HD turbulence has been explored in some detail. The energy is predominantly held within low wavenumber modes. Dissipation, on the other hand, occurs predominantly from the high wavenumber modes. Therefore, the decay rate does not generally depend on the details of the dissipation process. Rather, it is controlled by the efficiency of energy transfer from the low to high wavenumber modes due to vortex interactions, nonlinear wave interactions, or other processes. This leads either to the Kolmogorov decay rate $\eta = 10/7$ for the kinetic energy, accompanied by a growth in the external scale of the turbulence $\mathcal{L} \propto t^{2/7}$ [10], or to the law $\eta = 1 + (s-1)/(s+3)$ and $\mathcal{L} \propto t^{2/(s+3)}$, depending on the injected energy spectrum in the low wavenumber region ($P(k) \propto k^s$) and the spatial dimension D [11]. Hence, depending on s, values for the decay rate η as low as unity are predicted, much lower than Kolmogorov. However, these results are from studies of spatially free turbulence [12]. When turbulence is confined, a much higher rate of $\eta \to 2$ is found both experimentally [9] and with a mean field theory [13].

The decay behaviour of incompressible MHD turbulence, in contrast, is controversial. A two-dimensional (2D) analysis with constant mean square magnetic potential yields $\eta = 1$, a result indeed backed up by numerical studies in 2D [14]. Studies in 3D have yielded $\eta = 2/3$ [15] and $\eta = 0.8$ [16], although low-resolution numerical results [5,7] suggest $\eta \sim 1$.

Compressibility introduces an alternative type of complexity [17]. Nevertheless, the 3D decay problem has been modelled numerically [18]. Although the evolution of the spectral development and spatial structures was explored there, the decay rate was only treated in passing, and definitive results are hard to derive.

Unlike terrestrial turbulence, astrophysical turbulence usually involves full MHD compressible flow. Numerical models of one-dimensional (1D), isothermal, compressible, strongly magnetized, decaying and forced turbulence have been performed by [19], who found decay rates rather lower than those discussed above. A recent 3D study [20] broke new ground by examining both weakly and strongly magnetized isothermal, compressible turbulence; however the rather low energy decay rates shown there were almost entirely dependent on the initial conditions chosen, as explained in [21].

b. Numerical Techniques For our HD models of strongly supersonic turbulence we use two entirely different HD methods—a second-order, Eulerian, finite-difference code, and a smoothed particle hydrodynamics (SPH) code—while for our MHD models we use only the finite-difference code.

This finite-difference code is the well-tested MHD code ZEUS [22], which uses second-order [23] advection, and a consistent transport algorithm for the magnetic fields [24]. It resolves shocks using a standard von Neumann artificial viscosity, but otherwise includes no explicit viscosity, relying on numerical viscosity to provide dissipation at small scales. This should certainly be a reasonable approximation for shock-dominated flows, as most dissipation occurs in the shock fronts, where the artificial viscosity dominates in any case. The relative simplicity of this Eulerian formulation allows us to perform resolution studies showing that our major results are, in fact, independent of the resolution, and thus of the strength of numerical viscosity.

SPH is a particle based approach to solving the HD equations [25], in which the system is represented by an ensemble of particles, each carrying mass, momentum, and fluid properties such as pressure, temperature, and internal energy. We used the special-purpose processor GRAPE to accelerate computation of nearest-neighbor lists [26], allowing models with as many as 350,000 particles.

c. Initial Conditions We chose initial conditions for our models inspired by the popular idea that setting up velocity perturbations with an initial power spectrum $P(k) \propto k^\alpha$ in Fourier space similar to that of developed turbulence would be in some way equivalent to starting with developed turbulence [20,18]. Observing the development of our models, it became clear to us that, especially in the supersonic regime, the loss of phase information in the power spectrum allows extremely different gas distributions to have the same power spectrum. For example, supersonic, HD turbulence has been found in simulations [18] to have a power spectrum $\alpha = -2$. However, any single, discontinuous shock wave will also have such a power spectrum, as that is simply the Fourier transform of a step function, and taking the Fourier transform of many shocks will not change this power law. Nevertheless, most distributions with $\alpha = -2$ do not contain shocks.

After experimentation, we decided that the quickest way to generate fully developed turbulence was with perturbations having a flat power spectrum $\alpha = 0$ with a cutoff at $k_{\rm max} = 8$, and no long-wavelength rise in power (that is, the low-wavenumber power index s is undefined). We set up velocity perturbations drawn from a Gaussian random field fully determined by its power spectrum in Fourier space following the standard procedure: for each wavenumber $\mathbf{k}$ we randomly select an amplitude from a Gaussian distribution centered on zero and with width $P(k) = P_0 k^\alpha$ with $k = |\mathbf{k}|$, and a phase between zero and 2π. We then transform the field back into real space to obtain the velocity in each zone. This is done independently for each velocity component. For the SPH calculation the velocities defined on the grid are assigned onto individual particles using the "cloud-in-cell" scheme [27]. In all of our models we take $c_{\rm s} = 0.1$, initial density $\rho_0 = 1$, and we use a periodic grid with sides $L = 2$ centered on the origin. These parameter choices define our unit system. Our choice of periodic boundary conditions corresponds to the case of free turbulence discussed above, at least initially. Thereafter, the appropriate treatment is less clear.

d. One-Dimensional Results To verify our numerical methods, we reproduced the 1D, MHD results of Gammie & Ostriker [19]. Fig. 1*a* shows the results of a resolution study comparable to their Figure 1, with $M = 5$, initial uniform field parallel to the x-axis, and initial rms Alfvén number $A = v_{\rm rms}/v_{\rm A} = 1$, where $v_{\rm A}^2 = B^2/4\pi\rho_0$. Note that $t = 20$ in our units corresponds to $t = 1$ in theirs. Aside from a rather faster convergence rate in our study, attributable to the details of our choice of initial conditions, we reproduce excellently their result: a decrease in wave energy $E_{\rm wave} = E_{\rm K} + (B_{\rm y}^2 + B_{\rm z}^2)/8\pi$ by a factor of five in one sound-crossing time $L/c_{\rm s}$.

We then extended our study by examining the equivalent HD problem, as shown in Fig. 1*c*, only to find that the decay rate of HD turbulence in 1D is significantly *slower* than that of MHD turbulence. This appears to be due to the sweeping up of slower shocks by faster ones in the HD case, resulting in pure Bergers turbulence, with linear velocity profiles between widely separated shocks exactly as predicted [28]. The result is that there are very few dissipative regions, and energy is only lost very slowly. In contrast, multiple wave interactions occur in the MHD case producing many dissipative regions and so faster dissipation.

Finally we compared 1D models with 256 zone resolution to equivalent 3D models with 256^3 zones. The 3D model loses energy far faster than the 1D model in both the HD case shown in the thick lines in Fig. 1*d* and the MHD case shown in Fig. 1*b*. The increased number of degrees of freedom available in 3D produces more shocks and interaction regions, resulting in increased energy dissipation.

e. Three-Dimensional Results We next performed resolution studies using ZEUS for three different cases with no field, weak field and strong field as described in Fig. 2, and summarized in Table I. The weak field models have an initial ratio of thermal to magnetic pressure $\beta = 2$, while the strong field models have $\beta = 0.08$. We ran the same HD model with the SPH code to demonstrate that our results are truly independent of the details of the viscous dissipation, and so that our lack of an explicit viscosity does not affect our results. We also ran two models (R, S) with adiabatic index $\gamma = 1.4$, and an isothermal model (T) with initial $M = 0.1$ to provide a point of direct comparison between our results and those for incompressible, Navier-Stokes turbulence.

The kinetic energy decay curves for the four resolution studies are shown in Fig. 2. For each of our runs we performed a least-squares fit to the power-law portion of the kinetic energy decay curves, and report the corresponding decay rate η in Table I. These results appear converged at the 5–10% level; it is very reassuring that the different numerical methods converge to the same result for the HD case.

We find that highly compressible, isothermal turbulence (Model D) decays somewhat more slowly, with $\eta = 0.98$, than less compressible, adiabatic turbulence (Model R), with $\eta = 1.2$, or than incompressible turbulence (Model T), with $\eta = 1.1$ (also see [9,13]). Adding magnetic fields (Models L, Q, and S) decreases the decay rate somewhat further in the isothermal case to $\eta \sim 0.9$, with very slight dependence on the field strength or adiabatic index.

f. Conclusions We can draw conclusions for turbulence theory from our models that have significant astrophysical implications. What we find remarkable is how closely our results resemble the incompressible results, despite the difference in dissipation mechanisms. In incompressible hydrodynamics, kinetic energy is dissipated in vortexes at the smallest scales while in supersonic compressible turbulence, kinetic energy is dissipated in shock waves, and in MHD turbulence kinetic energy is dissipated in the interactions of nonlinear Alfvén waves, yet the resulting decay rates differ only slightly. The difference between our 1D and 3D HD results suggests that somehow the space density of dissipative regions is the determining factor, and that in 3D it is somehow quite independent of the detailed physics.

The clear astrophysical implication of these models is that even strong magnetic fields, with the field in equipartition with the kinetic energy, cannot prevent the decay of turbulent motions on dynamical timescales far shorter than the observed lifetimes of molecular clouds [29]. The significant kinetic energy observed in molecular cloud gas must be supplied more or less continuously. If turbulence supports molecular clouds against star formation, it must be constantly driven, by stellar outflows [30], photoionization [31,32], galactic shear [33], or some combination of these or other sources.

Some computations presented here were performed at the Rechenzentrum Garching of the MPG. ZEUS was used courtesy of the Laboratory for Computational Astrophysics at the NCSA. MDS thanks the DFG for financial support.

REFERENCES

* Email addresses: mordecai, burkert, klessen@mpia-hd.mpg.de
† Email address: smith@astro.uni-wuerzburg.de

[1] For an overview of molecular cloud physics and observations, see reviews by B. G. Elmegreen and by L. Blitz in *Protostars and Planets III*, edited by E. H. Levy and J. I. Lunine (University of Arizona Press, Tucson, 1993), p. 97 and 125, respectively

[2] L. Blitz and F. H. Shu, Astrophys. J. **238**, 148 (1980)

[3] M. Arons and C. Max, Astrophys. J. **196**, L77 (1975). Also see [19] and references therein.

[4] D. Biskamp, *Nonlinear Magnetohydrodynamics* (Cambridge University Press, Cambridge, England, 1994).

[5] M. Hossain, P. Gray, D. Pontius, W. Matthaeus, and S. Oughton, Phys. Fluids **7**, 2886 (1995).

[6] H. Politano, A. Pouquet, and P. L. Sulem in *Small-Scale Structures in Fluids and MHD*, edited by M. Meneguzzi, A. Pouquet, and P. L. Sulem, Springer-Verlag Lecture Notes in Physics Vol. 462 (Springer-Verlag, Berlin, 1995), p. 281.

[7] S. Galtier, H. Politano, and A. Pouquet, Phys. Rev. Lett. **79**, 2807 (1997).

[8] G. Comte-Bellot and S. Corrsin, J. Fluid Mech. **25**, 657 (1966); Z. Warhaft and J. Lumley, J. Fluid Mech. **88**, 659 (1978).

[9] M. R. Smith, R. J. Donnelly, N. Goldenfeld, and W. F. Vinen, Phys. Rev. Lett. **71**, 2583 (1993).

[10] A. N. Kolmogorov, Dokl. Acad. Nauk SSSR **30**, 9 (1941); C. F. von Weizsäcker, Z. Phys. **124**, 614 (1948); L. D. Landau and E. M. Lifshitz, *Fluid Mechanics* (Pergamon Press, Oxford, 1959), p. 143.

[11] M. Lesieur, *Turbulence in Fluids, 3rd Ed.* (Kluwer Academic Publishers, Dordrecht, 1997).

[12] K. R. Sreenivasan, S. Tavoularis, R. Henry, S. Corrsin, J. Fluid Mech. **100**, 597, (1980).

[13] D. Lohse, Phys. Rev. Lett. **73**, 3223 (1994).

[14] D. Biskamp and H. Welter, Phys. Fluids B **1**, 1964 (1989).

[15] T. Hatori, J. Phys. Soc. Japan **53**, 2539 (1984).

[16] R. Kinney, J.C. Mc Williams, & T. Tajima, *Phys. Plasmas*, **2**, 3623 (1995).

[17] S. K. Lele, Ann. Rev. Fluid Mech. **26**, 211 (1994).

[18] D. H. Porter, A. Pouquet, and P. R. Woodward, Phys. Rev. Lett. **68**, 3156 (1992); D. H. Porter, A. Pouquet, and P. R. Woodward, Phys. Fluids **6**, 2133 (1994).

[19] C. F. Gammie and E. C. Ostriker, Astrophys. J. **466**, 814 (1996).

[20] P. Padoan, and Å. Nordlund, Astrophys. J., submitted (1997), astro-ph/9703110.

[21] M.-M. Mac Low in press in *The Orion Nebula Revisited*, edited by M. J. McCaughrean and A. Burkert (San Francisco, Publ. Astron. Soc. Pacific, 1998), astro-ph/9711349.

[22] J. M. Stone and M. L. Norman, Astroph. J. **80**, 753 (1992); J. M. Stone and M. L. Norman, Astroph. J. **80**, 791 (1992).

[23] B. van Leer, J. Comput. Phys. **23**, 276 (1977).

[24] C. Evans, and J. F. Hawley, Astrophys. J. **33**, 659 (1988).

[25] Reviews of the SPH method are given by W. Benz in *The Numerical Modelling of*

Nonlinear Stellar Pulsations, edited by J. R. Buchler (Kluwer, Dordrecht, Netherlands, 1990), p. 269, and by J. J. Monaghan, Ann. Rev. Astron. Astroph. **30**, 543 (1992).
[26] The GRAPE project is described by T. Ebisuzaki, J. Makino, T. Fukushige, M. Taiji, D. Sugimoto, T. Ito, and S. Okumura, Publ. Astron. Soc. Japan **45**, 269 (1993); and the application to SPH is described in M. Steinmetz, M. N. Roy. Astron. Soc. **278**, 1005 (1996).
[27] R. W. Hockney and J. W. Eastwood, *Computer Simulation Using Particles* (Institute of Physics, Bristol, England, 1988)
[28] See p. 239 of [11].
[29] This was implied, though not emphasized, by the analytic study of E. G. Zweibel, and K. Josafattson, Astrophys. J. **270**, 511 (1983), as well as by the numerical study of [20], though with the problems discussed in paragraph *a*.
[30] e. g. J. Silk and C. Norman, in *Interstellar Molecules, IAU Symposium 87*, edited by B. H. Andrew (Reidel, Dordrecht, 1980), p. 165.
[31] C. F. McKee, Astrophys. J. **345**, 782 (1989); F. Bertoldi and C. F. McKee, in *Amazing Light*, edited by R. Y. Chiao (Springer, New York, 1996), p. 41.
[32] E. Vazquez-Semadeni, T. Passot, and A. Pouquet, Astrophys. J., **441**, 702 (1995).
[33] R. C. Fleck, Jr., Astrophys. J. **246**, L151 (1981).

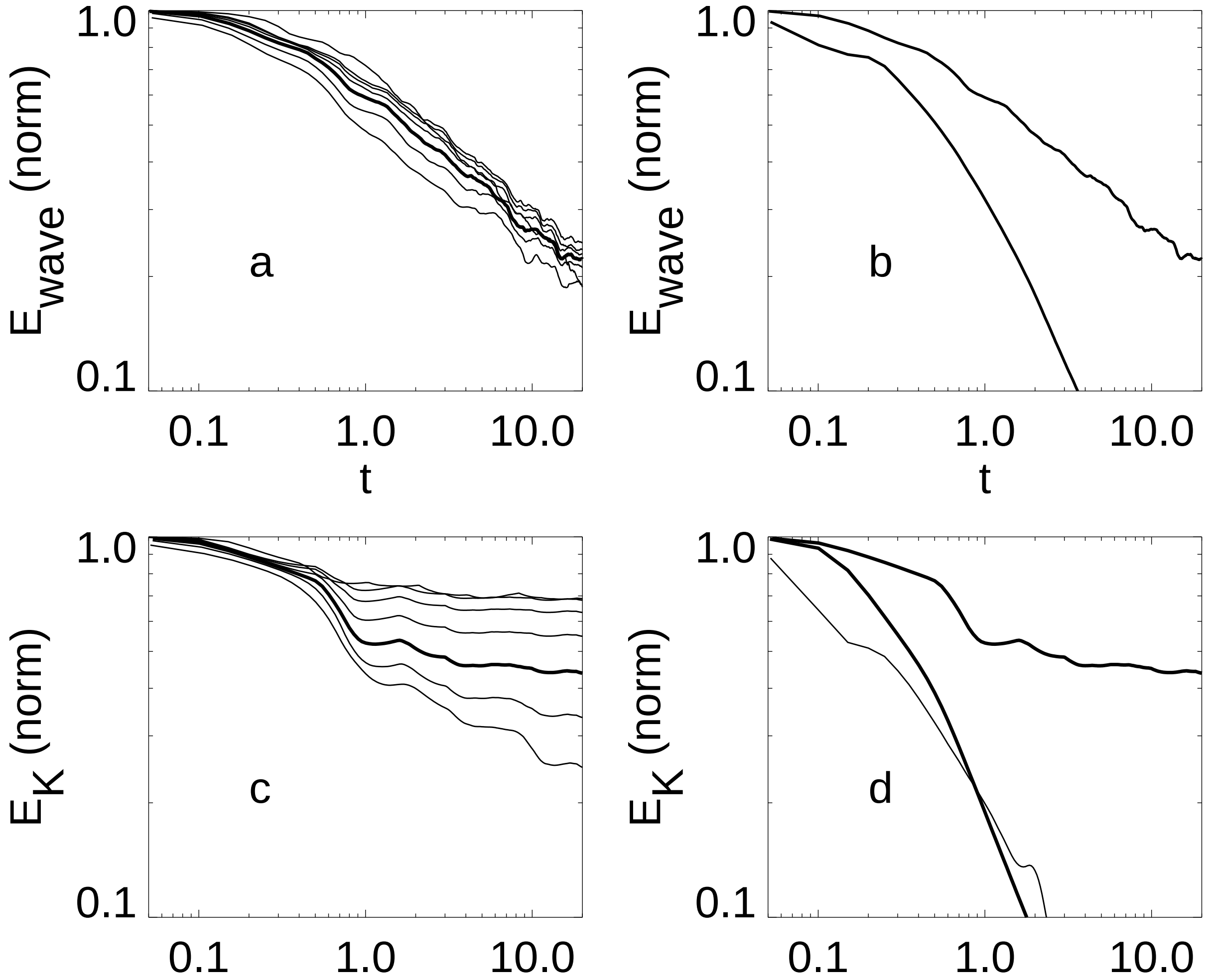

FIG. 1. Isothermal, $M = 5$ models with ZEUS. *a)* Wave energy decay of MHD models with $A = 1$ and resolutions ranging from 32 to 4096 zones; the 256 zone model is highlighted. *b)* Comparison of the same 256 zone 1D MHD model (*upper line*) to 256^3 zone 3D MHD Model Q (*lower line*). *c)* Kinetic energy decay of HD models with resolutions ranging from 32 (*lowest*) to 4096 (*highest*) zones; the 256 zone model is highlighted. *d)* Comparison of the same 256 zone 1D HD model (*upper thick line*) to 256^3 zone HD Model D (*lower thick line*) , and to 256^3 zone MHD Model Q (*thin line*)

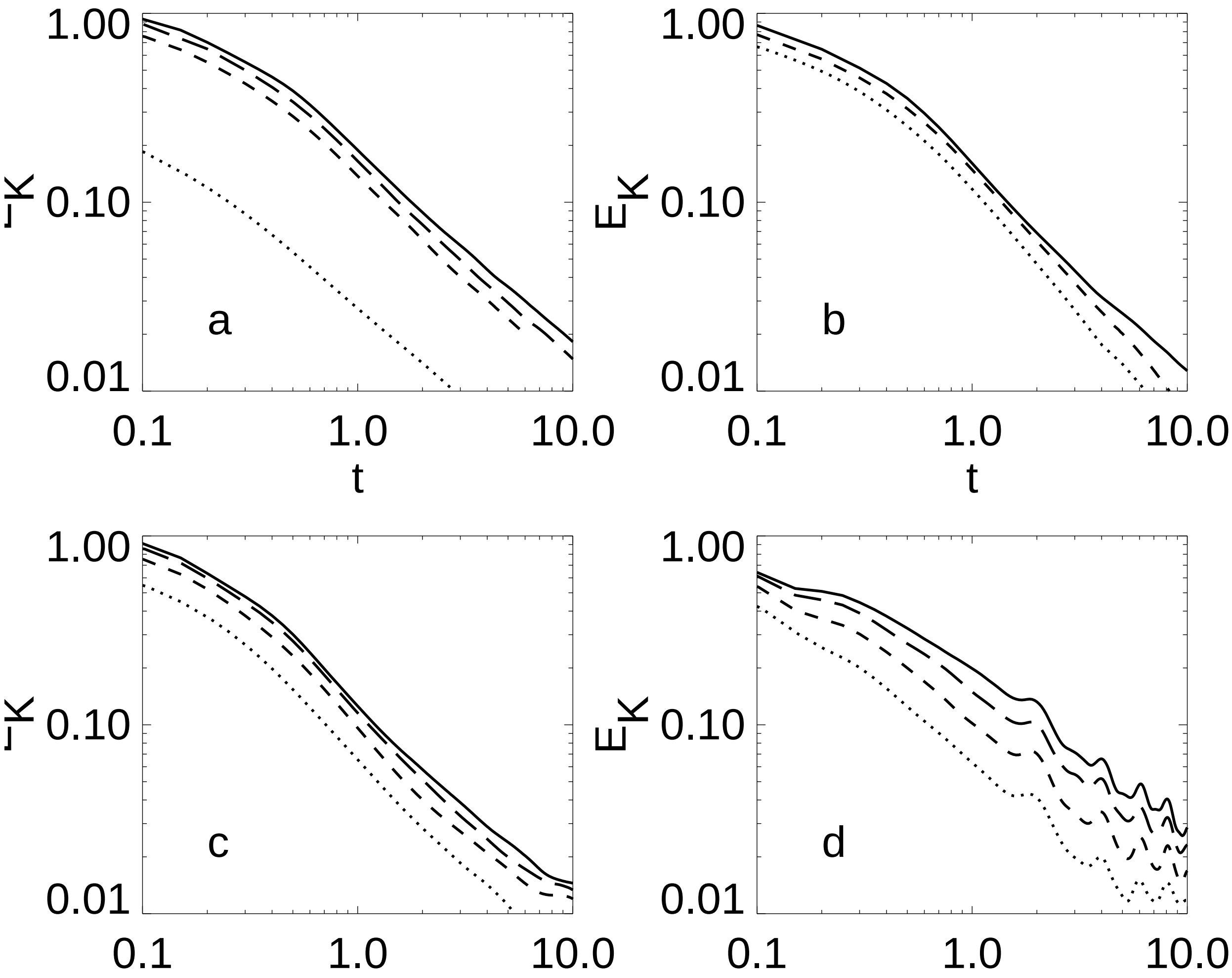

FIG. 2. 3D resolution studies for M=5, isothermal models. ZEUS models have 32^3 (*dotted*), 64^3 (*short dashed*), 128^3 (*long dashed*), or 256^3 (*solid*) zones, while the SPH models have 7000 (*dotted*), 50,000 (*short dashed*), or 350,000 (*solid*) particles. Panels show *a)* HD runs with ZEUS, *b)* HD runs with SPH, *c)* $A = 5$ MHD runs with ZEUS, and *d)* $A = 1$ MHD runs with ZEUS.

TABLES

TABLE I. Power law of kinetic energy decay η (with formal errors from the least squares fits) for the 3D models discussed. Initial rms Mach number M and Alfvén number A, and adiabatic index γ are given, along with the resolution (in zones per side or thousands of particles) and code used. Boldface indicates highest resolution.

Mod	code	res	γ	M	A	η
A	ZEUS	32	1	5	∞	0.93 $\pm$ 0.001
B	ZEUS	64	1	5	∞	1.1 $\pm$ 0.003
C	ZEUS	128	1	5	∞	1.0 $\pm$ 0.002
D	**ZEUS**	**256**	**1**	**5**	$\boldsymbol{\infty}$	**0.98$\pm$ 0.001**
E	SPH	7	1	5	∞	1.3 $\pm$ 0.005
F	SPH	50	1	5	∞	1.2 $\pm$ 0.001
G	**SPH**	**350**	**1**	**5**	$\boldsymbol{\infty}$	**1.1 $\pm$ 0.004**
H	ZEUS	32	1	5	5	0.89$\pm$ 0.02
J	ZEUS	64	1	5	5	0.80$\pm$ 0.01
K	ZEUS	128	1	5	5	0.86$\pm$ 0.01
L	**ZEUS**	**256**	**1**	**5**	**5**	**0.91$\pm$ 0.006**
M	ZEUS	32	1	5	1	0.67$\pm$ 0.02
N	ZEUS	64	1	5	1	0.80$\pm$ 0.02
P	ZEUS	128	1	5	1	0.83$\pm$ 0.02
Q	**ZEUS**	**256**	**1**	**5**	**1**	**0.87$\pm$ 0.02**
R	**ZEUS**	**256**	**1.4**	**5**	$\boldsymbol{\infty}$	**1.2 $\pm$ 0.006**
S	**ZEUS**	**256**	**1.4**	**5**	**1**	**0.94$\pm$ 0.009**
T	**ZEUS**	**256**	**1**	**0.1**	$\boldsymbol{\infty}$	**1.1 $\pm$ 0.007**